Non-linear neutron star oscillations viewed as deviations from an equilibrium state

Ulrich Sperhake

Department of Physics, Section of Astrophysics,
Aristotle University of Thessaloniki, 54124 Thessaloniki, Greece
Faculty of Mathematical Studies,
University of Southampton, Southampton SO17 1BJ, UK,
email: sperhake@astro.auth.gr

Abstract

A numerical technique is presented which facilitates the evolution of non-linear neutron star oscillations with a high accuracy essentially independent of the oscillation amplitude. We apply this technique to radial neutron star oscillations in a Lagrangian formulation and demonstrate the superior performance of the new scheme compared with "conventional" techniques. The key feature of our approach is to describe the evolution in terms of deviations from an equilibrium configuration. In contrast to standard perturbation analysis we keep all higher order terms in the evolution equations and thus obtain a fully non-linear description. The advantage of our scheme lies in the elimination of background terms from the equations and the associated numerical errors. The improvements thus achieved will be particularly significant in the study of mildly non-linear effects where the amplitude of the dynamic signal is small compared with the equilibrium values but large enough to warrant non-linear effects. We apply the new technique to the study of non-linear coupling of eigenmodes and non-linear effects in the oscillations of marginally stable neutron stars. We find non-linear effects in low amplitude oscillations to be particularly pronounced in the range of modes with vanishing frequency which typically mark the onset of instability.

Keywords: neutron star oscillations, non-linearity, numerical techniques.

1 Introduction

The study of neutron star oscillations has long since been a topic of considerable scientific interest. Perturbation techniques have been used as early as the 1960s for the investigation of radial oscillations and the stability properties of neutron stars [3]. In more recent years the interest in neutron star simulations has further intensified due to the discovery of the gravitational radiation driven instability of the r-modes [1]. A great deal of work has been spent on the development of non-linear, 3-dimensional, relativistic hydrodynamic simulations to investigate such scenarios (see e.g. [4] and references therein). One of the most important questions raised in connection with the r-mode instability concerns the efficiency with which energy is dissipated due to viscosity or non-linear effects. The numerical investigation of non-linear effects in this respect appears to be relying on codes which are not specifically designed to capture mildly non-linear effects in the low-amplitude regime. Results thus obtained have indicated a large saturation amplitude of order unity of the r-modes (see e.g. [5]) but have been called into question by studies which analytically take into account the non-linear mode-coupling and find significant non-linear interaction which prevents a further growth of the r-mode at amplitudes at least 4 orders of magnitude smaller [2]. In the context of simulating non-linear neutron star oscillations at rather small amplitudes it is interesting to note that the signature of the numerical truncation error caused by the intrinsic presence of background terms in the evolution equations has been observed in 3D non-linear evolutions [10]. While these authors find this error to decrease at second order with the grid-resolution and not to seriously affect their results, one has to bear in mind that the impact of the resulting spurious source terms will strongly depend on the amplitude of the dynamic signal. The smaller the deviations from the equilibrium configuration the more significant we expect the numerical

contamination to affect the simulations. It appears desirable therefore to have a numerical scheme where the error is determined solely by the amplitude of the dynamic signal as opposed to the equilibrium background. In section 2 and 3 we will elaborate on the numerical scheme presented in [9] and show how such an amplitude independent accuracy can be obtained by decomposing the numerical evolution into a static background and time dependent deviations from that background. After testing the resulting code we demonstrate the improvements by comparing numerical evolutions obtained with the new and a "conventional" scheme. In section 6 we use the code to investigate radial neutron star oscillations in an amplitude regime where the elimination of the above mentioned numerical errors is crucial and yet significant non-linear effects are present.

2 The "conventional" formulation

2.1 The equations for a dynamic spherically symmetric neutron star

In this paper we extend the work of [9] who have applied the idea of numerically evolving non-linear deviations from an equilibrium state to a truncated neutron star model with fixed outer boundary. The main reason for using such a simplified model were difficulties encountered at the surface of the star (see [8] for details). Here we use a Lagrangian approach which straightforwardly facilitates an exact treatment of the moving stellar surface. The derivation of the equations for a dynamic spherically symmetric neutron star was inspired by the work of [7]. We thus describe the spacetime in terms of the line element in polar slicing and Lagrangian gauge

$$ds^2 = \hat{\lambda}^2 \left(-1 + \frac{w^2}{\hat{\Gamma}} \right) dt^2 + 2 \frac{\hat{r}_{,x} \hat{\lambda} w}{\hat{\Gamma}} dt\, dx + \frac{\hat{r}_{,x}^2}{\hat{\Gamma}} dx^2 + \hat{r}^2 (d\theta^2 + \sin^2\theta\, d\phi^2). \tag{1}$$

Here $\hat{\lambda}$, $\hat{\Gamma}$ and $\hat{r}$ are functions of the spatial coordinate x and coordinate time t and we have defined the velocity of the fluid elements $w = \hat{r}_{,t}/\hat{\lambda}$. In this formulation the circumferential radius $\hat{r}$ is a time dependent variable whereas the "co-moving" spatial coordinate x labels the fluid elements. We model the matter as a perfect fluid at zero temperature with a polytropic equation of state $\hat{P} = K \hat{\rho}^\gamma$, where $\hat{P}$ and $\hat{\rho}$ are the pressure and total energy density and the polytropic exponent γ and K are constant parameters. The Lagrangian nature of our coordinate system is reflected in the 4-velocity u^α which has a non-vanishing time component only

$$u^\alpha = \left(\frac{1}{\hat{\lambda}\sqrt{1 - \frac{w^2}{\hat{\Gamma}}}},\ 0,\ 0,\ 0 \right). \tag{2}$$

Finally the energy momentum tensor for a perfect fluid is given by

$$T_{\alpha\beta} = (\hat{\rho} + \hat{P}) u_\alpha u_\beta + \hat{P} g_{\alpha\beta}. \tag{3}$$

In order to write the Einstein field equations $G_{\alpha\beta} = 8\pi T_{\alpha\beta}$ and the equations of conservation of energy-momentum $\nabla_\alpha T_\beta{}^\alpha = 0$ it is convenient to introduce the function $\hat{N}$ by

$$\hat{\Gamma} = 1 - 2\hat{N}\hat{r}, \tag{4}$$

which is related to the more commonly used mass function by $\hat{m} = \hat{r}^2 \hat{N}$ and thus behaves like $O(x)$ at the origin as opposed to the $O(x^3)$ behavior of $\hat{m}$ which we find to cause a larger error in the Oppenheimer-Snyder dust-collapse of section 4. The equations can then be written in the form

$$\frac{\hat{\lambda}_{,x}}{\hat{\lambda}} = \frac{\hat{r}_{,x}}{\hat{\Gamma}} \left(\hat{N} + 4\pi\hat{r} \frac{w^2\hat{\rho} + \hat{\Gamma}\hat{P}}{\hat{\Gamma} - w^2} \right), \tag{5}$$

$$\hat{N}_{,x} = -2\frac{\hat{r}_{,x}}{\hat{r}}\hat{N} + 4\pi\hat{r}_{,x} \frac{\hat{\Gamma}\hat{\rho} + w^2\hat{P}}{\hat{\Gamma} - w^2}, \tag{6}$$

$$\hat{r}\hat{N}_{,t} = -2\hat{\lambda} w \hat{N} - 4\pi\hat{r}\hat{\lambda} w \hat{P}, \tag{7}$$

$$\hat{r}_{,t} = \hat{\lambda} w, \tag{8}$$

$$0 = (\hat{\Gamma} - w^2)^2 \frac{\hat{P}_{,x}}{\hat{r}_{,x}} + \hat{P}_{,t} \frac{w}{\hat{\lambda}} (\hat{\Gamma} - w^2) + (\hat{\rho} + \hat{P}) \left[\hat{\Gamma} \frac{w_{,t}}{\hat{\lambda}} + (\hat{\Gamma} - 2w^2) \left(\hat{N} + 4\pi\hat{r}\hat{P} \right) \right]. \tag{9}$$

2.2 Boundary conditions and initial data

For the numerical evolution of the system (4)-(9) we need to prescribe boundary conditions. At the origin $x = 0$ we require $\hat{r} = 0$, $w = 0$, $\hat{N} = 0$ which follows from spherical symmetry and demanding that there be no conical singularity at the origin. At the surface of the star we have $\hat{P} = 0$ and $\hat{\lambda} = \sqrt{1 - 2\hat{N}\hat{r}}$. The first condition is the definition of the stellar surface and translates into $\hat{\rho} = 0$ for the polytropic equation of state while the second condition matches the line element (1) to an exterior Schwarzschild metric.

For the prescription of initial data and the development of our new numerical formulation in section 3 it is essential to discuss the static and the linearized limit of the evolution system (5)-(9). The static limit describes spherically symmetric neutron stars in equilibrium and is obtained by setting all time derivatives to zero in Eqs. (5)-(9). We thus obtain the well known Tolman-Oppenheimer-Volkoff (TOV) equations

$$\frac{\lambda_{,x}}{\lambda} = \frac{r_{,x}}{\Gamma}\left(N + 4\pi r P\right), \tag{10}$$

$$N_{,x} = -2\frac{r_{,x}}{r}N + 4\pi r_{,x}\rho, \tag{11}$$

$$0 = \Gamma P_{,x} + r_{,x}(\rho + P)\left(N + 4\pi r P\right), \tag{12}$$

where $\Gamma = 1 - 2Nr$. We note that we have omitted the "hat" from these time independent equilibrium variables in order to distinguish them from the total quantities. The boundary conditions for the TOV equations are $N = 0$, $r = 0$ at the origin and $P = 0$ at the surface. We also use the background configuration to fix the Lagrangian coordinate x by the requirement $r_{,x} = C$, where the sound speed of the background model is defined by $C^2 = \partial P/\partial\rho$. This definition provides a high density of grid points in regions of small characteristic speeds (see [8] for details).

The linearized version of the evolution system around the TOV background is best formulated in terms of the rescaled displacement vector $\zeta = r^2\xi/\lambda$, where $\xi = \Delta r$ is the displacement of the fluid elements in terms of the circumferential radius. The linearized equations then lead to a self adjoint eigenvalue problem

$$\frac{1}{r_{,x}}\left(\frac{\Pi}{r_{,x}}\zeta_{,x}\right)_{,x} + (\omega^2 W + Q)\zeta = 0, \tag{13}$$

where

$$\Pi = C^2(\rho + P)\frac{\lambda^3}{\sqrt{\Gamma}r^2}, \tag{14}$$

$$W = (\rho + P)\frac{\lambda}{\sqrt{\Gamma}^3 r^2}, \tag{15}$$

$$Q = \frac{\lambda^3}{\sqrt{\Gamma}r^2}(\rho + P)\left[\left(\frac{\lambda_{,x}}{r_{,x}\lambda}\right)^2 + 4\frac{\lambda_{,x}}{r r_{,x}\lambda} - 8\pi\frac{P}{\Gamma}\right], \tag{16}$$

and the eigenvalue ω^2 is the square of the frequency of the associated eigenmode. From mathematical theorems it is known that this eigenvalue problem has an infinite number of solutions ζ_1, ζ_2,... with ordered eigenvalues $(\omega_1)^2 < (\omega_2)^2 < ....$ After appropriate rescaling the eigenfunctions form a complete orthonormal set, i.e.

$$\langle\zeta_i, \zeta_j\rangle := \int_0^{x_s} W\zeta_i\zeta_j dx = \delta_{i,j}, \tag{17}$$

and any function $f(x)$ with appropriate boundary conditions can be expanded in a series

$$f(x) = \sum_i A_i\zeta_i(x), \tag{18}$$

where $A_i = \langle f, \zeta_i\rangle$. The boundary conditions for the eigenvalue problem are given by the requirement that ζ vanishes at the origin and remains finite at the surface. From a numerical point of view both the TOV equations (10)-(12) and the eigenvalue problem (13) are two point boundary value problems which we solve with a second order relaxation method. The resulting eigenmode profiles serve us as initial data for the non-linear evolutions.

3 A "non-linear perturbative" formulation

In this section we will demonstrate how a fully non-linear formulation of the dynamic problem in terms of deviations from the TOV-background eliminates the numerical truncation error of the background intrinsic to the "conventional formulation" of the previous section. It is convenient, however, to first illustrate in the case of a simple toy equation the motivation of our approach.

3.1 The non-linear "perturbative scheme": a toy equation

Let us assume for this purpose that a physical system is described in terms of variables $\hat{f}$, $\hat{g}$ and $\hat{h}$ which all depend on spatial position x and time t. We further assume that one of the equations governing the system is

$$\hat{h}_{,t} = \hat{h}_{,x} + \hat{f}\hat{g}, \tag{19}$$

and that there exist a non-trivial equilibrium of the system described by $f(x)$, $g(x)$ and $h(x)$ which obey the time independent version of Eq. (19)

$$h_{,x} + fg = 0. \tag{20}$$

We note again the omission of the "hat" for the equilibrium functions. We can now decompose the time dependent functions into static background contributions and time dependent deviations according to $\hat{f}(t,x) = f(x) + \Delta f(t,x)$ and likewise for $\hat{g}$ and $\hat{h}$. Inserting this into Eq. (19) we obtain the equivalent equation

$$\Delta h_{,t} = \Delta h_{,x} + f\Delta g + g\Delta f + \Delta f \Delta g + (h_{,x} + fg). \tag{21}$$

It is the term in brackets on the right hand side which motivates our reformulation of the problem. From Eq. (20) we know that this term vanishes identically. Numerically, however, this will only be satisfied up to a finite error which represents a spurious source term in the evolution of Δh. The severeness of this effect depends on the magnitude of the numerical error i.e. the grid resolution and the relative size of the deviations Δf, Δg, Δh with respect to the background values. This effect is intrinsic to any numerical scheme based on a "conventional formulation" such as that of section 2.
By virtue of our decomposition, however, we can use Eq. (20) to eliminate the problematic terms *prior* to the numerical evolution and instead of Eq. (21) use

$$\begin{aligned} \Delta h_{,t} &= \Delta h_{,x} + f\Delta g + g\Delta f + \Delta f \Delta g & (22)\\ &= \Delta h_{,x} + f\Delta g + \hat{g}\Delta f. & (23) \end{aligned}$$

It is important to note that in contrast to standard perturbation techniques we keep all terms of higher order in the deviations, such as $\Delta f \Delta g$, so that our formulation is equivalent to the original non-linear problem.

3.2 The "non-linear perturbative" equations for the dynamic neutron star

We will now reformulate the system of evolution equations (4)-(9) in terms of deviations from the TOV equilibrium background. For this purpose we decompose the variables according to $\hat{\lambda}(t,x) = \lambda(x) + \Delta\lambda(t,x)$ and likewise for $\hat{N}$ and $\hat{\Gamma}$. In the case of the circumferential radius we depart from this notational convention and instead write $\hat{r}(t,x) = r(x) + \xi(t,x)$ since the radial displacement is commonly denoted by ξ in the literature. After eliminating all zero order terms by using the TOV equations (10)-(12) the evolution equations can be written as

$$\Delta\Gamma - 1 + 2\hat{N}\xi + 2\Delta N r = 0, \tag{24}$$

$$\begin{aligned} &\hat{\Gamma}^2\Delta\lambda_{,x} + \Delta\Gamma(2\Gamma + \Delta\Gamma)\lambda_{,x} - (\xi_{,x}\lambda\Gamma + \hat{r}_{,x}\Delta\lambda\Gamma + \hat{r}_{,x}\hat{\lambda}\Delta\Gamma)(N + 4\pi rP)\\ &+ w^2\left[-\hat{\Gamma}\hat{\lambda}_{,x} + \hat{r}_{,x}\hat{\lambda}(\hat{N} - 4\pi\hat{r}\hat{\rho})\right] - \hat{r}_{,x}\hat{\lambda}\hat{\Gamma}\left[\Delta N + 4\pi(\xi P + \hat{r}\Delta P)\right] = 0, \end{aligned} \tag{25}$$

$$\begin{aligned} &- w^2(\hat{r}\hat{N}_{,x} + 2\hat{r}_{,x}\hat{N} + 4\pi\hat{r}\hat{r}_{,x}\hat{P}) + \Delta\Gamma(\hat{r}\hat{N}_{,x} + 2\hat{r}_{,x}\hat{N} - 4\pi\hat{r}\hat{r}_{,x}\hat{\rho})\\ &+ \Gamma\left[\xi N_{,x} + \hat{r}\Delta N_{,x} + 2\xi_{,x}N + 2\hat{r}_{,x}\Delta N - 4\pi(\xi\rho r_{,x} + \hat{r}\xi_{,x}\rho + \hat{r}\hat{r}_{,x}\Delta\rho)\right] = 0, \end{aligned} \tag{26}$$

$$\hat{r}\Delta N_{,t} + 2\hat{\lambda}w(\hat{N} + 2\pi\hat{r}\hat{P}) = 0, \tag{27}$$

$$\xi_{,t} - \hat{\lambda}w = 0, \tag{28}$$

$$\hat{\lambda}(-2\hat{\Gamma}w^2+w^4)\hat{P}_{,x}+\hat{r}_{,x}w\Omega^2\hat{P}_{,t}+(\hat{\rho}+\hat{P})\hat{r}_{,x}\left[\hat{\Gamma}w_{,t}-2\hat{\lambda}w^2(\hat{N}+4\pi\hat{r}\hat{P})\right]$$
$$+(\Delta\lambda\Gamma+\hat{\lambda}\Delta\Gamma)\left[\hat{\Gamma}\hat{P}_{,x}+(\hat{\rho}+\hat{P})\hat{r}_{,x}(\hat{N}+4\pi\hat{r}\hat{P})\right]+\lambda\Gamma\left\{\Delta\Gamma P_{,x}+\hat{\Gamma}\Delta P_{,x}\right. \tag{29}$$
$$\left.+\left[(\Delta\rho+\Delta P)r_{,x}+(\hat{\rho}+\hat{P})\xi_{,x}\right](N+4\pi rP)+(\hat{\rho}+\hat{P})\hat{r}_{,x}(\Delta N+4\pi\xi P+4\pi\hat{r}\Delta P)\right\}=0.$$

We solve this system of evolution equations with an implicit, second order in space and time numerical scheme similar to the Crank-Nicholson scheme (see [8] for details).

4 Testing the code

We have tested the resulting numerical code in three independent ways which cover a large range of amplitudes of the deviations. First we consider the linear regime. For this purpose we calculate a background neutron star model with polytropic parameters $\gamma = 2$, $K = 150\,\mathrm{km}^2$, mass $M = 1.48\,M_\odot$ and radius $R = 11.3\,\mathrm{km}$. This model is located well on the stable branch. We choose initial data in the form of the third eigenmode with an initial amplitude of 10 cm. This amplitude is sufficiently small that we expect the evolution to be very well approximated by the solution of the linearized problem (13). For such evolutions we find that the numerical solution reproduces the analytic solution with a relative point wise error of about 10^{-3} for 200 grid points. Secondly we have performed a convergence analysis for evolving the second eigenmode with an initial amplitude of 50 m. This corresponds to the mildly non-linear regime, where we observe non-linear effects (cf. section 6), but no shock formation is observed for initial data with sufficiently weak spatial variation. We have calculated numerical solutions using 400, 800 and 1600 grid points and find the resulting convergence factors for the dependent variables ξ, w, ΔN, $\Delta\rho$ and $\Delta\lambda$ to be in good agreement with the expected second order convergence. For the third test we have simulated the collapse of a spherically symmetric, initially homogeneous dust cloud, i.e. a fluid with zero pressure. The analytic solution for this scenario has been derived by [6] and the expressions in terms of our variables as well as more details on all three tests can be found in [8]. We find our code to reproduce the analytic solution with a relative accuracy better than 10^{-3} for 800 grid points up to a time when the dust sphere has collapsed very close to its Schwarzschild radius. At this stage the "collapse of the lapse" freezes the evolution. It is only at these late, dynamically irrelevant stages that the steep gradients commonly observed in singularity avoiding slicing cause a deterioration of the accuracy of our code. With the exception of shock formation, the numerical treatment of which we postpone to a future publication, we thus find the code to perform equally well for arbitrary amplitudes.

5 Comparison with "conventional methods"

In order to compare the numerical schemes outlined in sections 2 and 3 we consider the evolution of the third eigenmode of the above model with an amplitude of 1 m using 200 grid points. For this amplitude the evolution should still be close to that predicted by the linearized equations, so that we expect the initial eigenmode profile to oscillate harmonically. In the analysis of non-linear coupling of eigenmodes, we will see that amplitudes of this order of magnitude will already give rise to measurable albeit very small non-linear effects. In Fig. 1 we show snapshots of the evolutions of the displacement ξ (left panel) and the energy density deviation $\Delta\rho$ (right panel). The dotted lines represent the initial data, the dashed lines the results obtained with our non-linear perturbative scheme of section 3 and the solid lines those obtained with the conventional scheme of section 2. The results demonstrate that the new scheme produces the expected oscillations while the "conventional" scheme leads to severely distorted profiles. The numerical noise visible in the solid curve of $\Delta\rho$ arises from the spurious formation of shocks near the stellar surface. It is important to note in this context that we have used the same code for both these numerical runs. In the first case we have used the TOV-background whereas in the second case we use a flat vacuum background, i.e. $\lambda = 1$, $N = 0$, $\rho = 0$. One straightforwardly shows that Eqs. (24)-(29) indeed reduce to the system (4)-(9) with the total variables $\hat{f}$ replaced by the deviations Δf or $1 + \Delta f$ in the case of λ. The only numerically significant difference between the two runs is therefore the presence or absence of the background error terms analogous to the term in brackets on the right hand side of Eq. (21). We conclude that the presence of these terms significantly contaminates the numerical evolution and gives rise to spurious numerical effects such as mode coupling

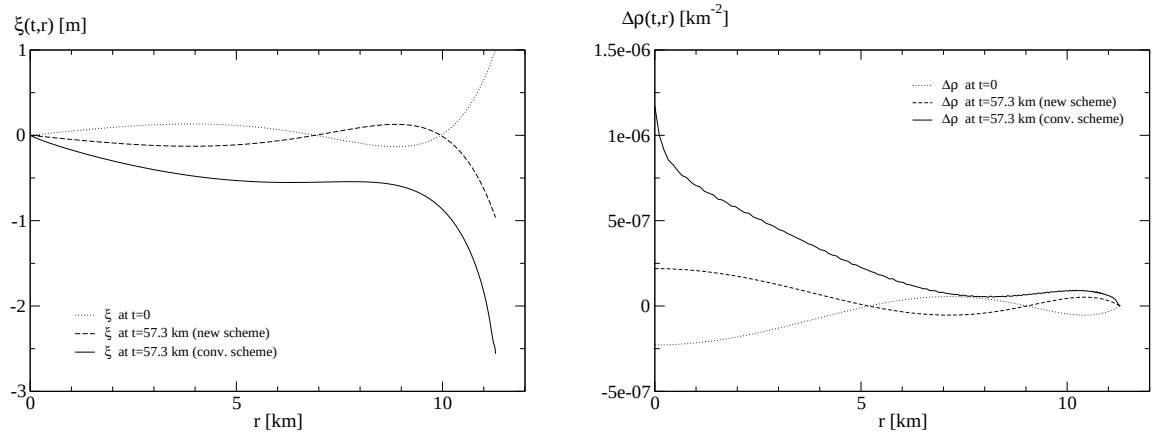

Figure 1: Snap shots of the evolution of ξ (right panel) and $\Delta\rho$ (left panel) obtained with a non-linear perturbative and a conventional scheme.

and shock formation. We find the significance of this effect to decrease with higher grid resolution and larger amplitude of the initial data. Our new scheme will therefore be particularly suitable for studying mildly non-linear effects at amplitudes notably smaller than the background values.

6 Applications

6.1 Non-linear coupling of eigenmodes

In section 1 we have already noted the importance of a detailed understanding of non-linear coupling of eigenmodes for addressing questions such as the saturation amplitudes of neutron star oscillations. Analytic studies of mode-coupling effects normally view the eigenmode coefficients A_i (cf. Eq. 18) as harmonic oscillators and the non-linear interaction between different modes is represented in the form of a series of driving terms with increasing order in the amplitudes which is truncated at second or third order (see e.g. [11]). While the investigation of neutron star oscillations in 3-dimensions such as r-modes is beyond the scope of our work, we will demonstrate in the case of radial oscillations that our scheme presents a numerical alternative to study non-linear coupling of eigenmodes without any restrictions due to the emission of higher order terms. For this purpose we consider the neutron star model of section 4 and provide initial data in the form of one isolated eigenmode. The index j of this mode and the initial amplitude given by the initial displacement of the stellar surface ξ_s in m from the equilibrium radius are the two free parameters. During the fully non-linear evolution we make use of Eq. (18) which enables us to expand the time dependent displacement function according to $\xi(t,x) = \sum_i A_i(t)\xi_i(x)$. The time dependent eigenmode coefficients are then given by $A_i(t) = \langle \xi(t,x), \xi_i(x) \rangle$ and can be calculated at each time step. In the amplitude range considered here we typically find these coefficients to oscillate with a frequency close to the value predicted by linear theory. We therefore measure the degree to which a mode is present in an evolution by taking the maximum of $|A_i(t)|$ which we denote by A_i. The integration time for these runs is $T \approx 4\,\mathrm{ms}$ which corresponds to about 10 oscillation periods of the fundamental mode. In Fig. (2) we show the eigenmode coefficients A_i of the first 5 eigenmodes thus obtained for $j = 2$ as a function of the initial surface displacement. The only mode initially present in these evolutions is the second mode and we find the corresponding eigenmode coefficient A_2 ("+" in the figure) to depend linearly on the initial surface displacement ξ_s. Other eigenmodes while not present in the initial data, are excited in the course of the non-linear evolution, so that we find non-zero values for the other A_i. We clearly see that the degree of excitation increases with the initial amplitude. A more detailed analysis reveals that the dependence of the A_i on ξ_s can be well approximated by power laws with integer index as shown in the figure. While A_1, A_3 and A_4 are well approximated by a quadratic power law, we find that A_5 grows like the cube of ξ_s. We have frequently observed that the excitation of higher order modes is modeled by larger integer power law indices, although we also find exceptions to this rule. A more systematic analysis of this dependency requires larger data sets and is postponed to future work. We stress the importance of the amplitude independent accuracy provided by our scheme for being able to measure these effects. The deviations of A_5 from the power

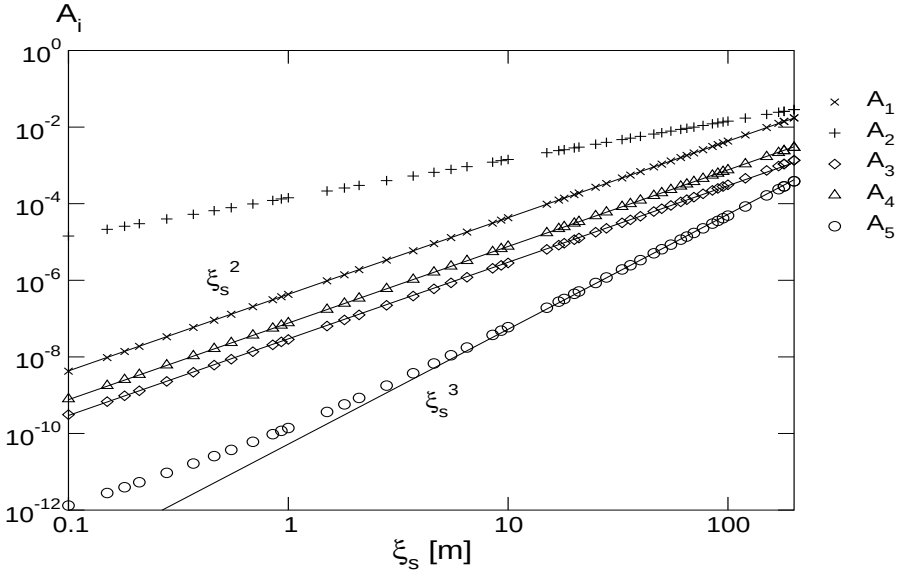

Figure 2: The eigenmode coefficients A_i are shown for initial data in the form the second eigenmode as a function of the initial amplitude ξ_s.

law behavior observed at small amplitudes are most likely caused by the accuracy limits encountered even when using our scheme with the large resolution of 3200 grid points.

6.2 Oscillations of marginally stable neutron stars

We have already seen that the benefits of our numerical scheme are most important when studying non-linear effects associated with rather small deviations from the equilibrium configuration. It is clear that such non-linear effects will be particularly pronounced if the linear first order terms in the evolution equations (25)-(29) largely cancel each other. In that case the higher order terms and the associated non-linear effects will dominate the evolution even for very small amplitudes of the dynamic signal. It has been known for a long time that the onset of dynamic instability of neutron stars to radial perturbations occurs at a point where the frequency of the fundamental eigenmode becomes zero (see e.g. [3]). Radial oscillations of neutron stars very close to the maximum of the mass-radius curve should therefore provide a fertile area of application for our numerical scheme. We consider a neutron star background model with the same equation of state as before, but a higher central density, so that the star has a mass only a fraction $6 \cdot 10^{-7}$ below the maximum mass $M_{\max} = 1.655\, M_\odot$. In Fig. (3) we show the surface displacement obtained for evolving the fundamental eigenmode with an initial amplitude of $+10$ (dashed curve) and $-10\,\mathrm{m}$ (solid curve). We note several deviations from the harmonic oscillations predicted by the linearized theory. First the oscillation amplitude as well as the frequency depend on the sign of the initial perturbation. Secondly the star does not oscillate around its equilibrium position (dotted curve) but around a larger radial position. Furthermore the oscillation of the solid curve (initial contraction) appears to be distorted relative to a purely harmonic shape. For larger amplitudes this feature becomes more prominent and distinct for both signs of the initial perturbation. Finally a quantitative analysis yields that both oscillation frequencies are significantly larger than the value predicted by linear theory. We have investigated this frequency shift in more detail by determining the frequencies of the non-linear evolutions via Fourier analysis over a wide range of amplitudes. The results are shown in the right panel of Fig. (3) and demonstrate that the frequencies of the non-linear evolutions ("$\times$") differ from the linearized value (dashed line) by up to one order of magnitude over the amplitude range considered here. As the amplitude goes to zero, we recover the value predicted by perturbation theory, but even for initial perturbations as small as 1 m we observe differences of several percent and a notable distortion of the oscillation profiles similar to Fig. (3). In contrast we have found excellent agreement between the frequencies for "ordinary" neutron stars located much further away from the stability limit. In such cases linear theory predicts frequencies which agree with our non-linear evolutions to less than 1 % for amplitudes well above 10 m. We conclude that the discrepancies observed for neutron stars near their stability limit are due to

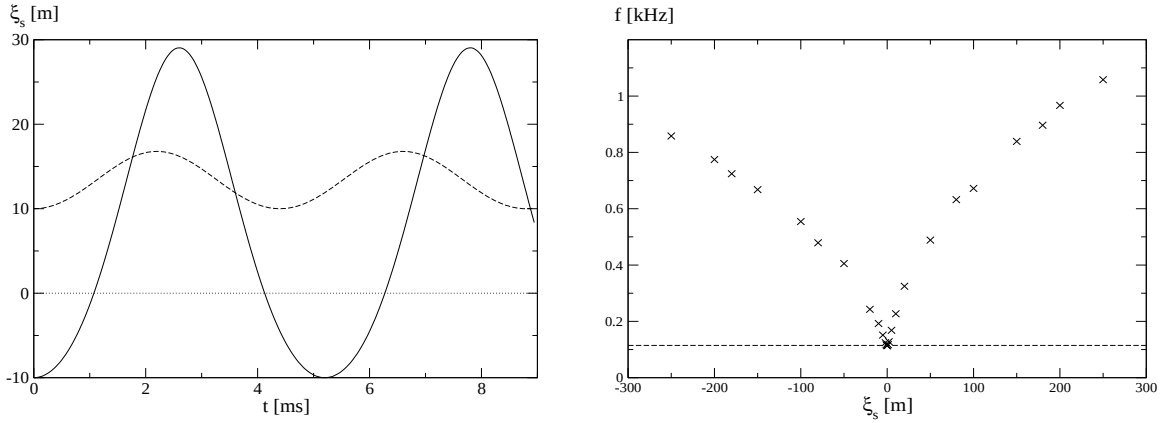

Figure 3: Left panel: The surface displacement of a marginally stable neutron star is shown as a function of time for an initial amplitude of +10 and −10 m. Right panel: The frequencies obtained from the non-linear evolutions of the fundamental eigenmode with initial amplitude ξ_s. The dashed curve marks the frequency predicted by linearized perturbation theory.

non-linear effects. We finally note that non-linear effects appear to increase the oscillation frequency away from the zero limit which represents the onset of instability. This indicates that non-linear effects may stabilize the neutron star. First runs obtained for neutron stars close to the stability limit but located on the unstable branch confirm this result. While small initial amplitude lead to a collapse of the star, the same initial data with larger amplitude give rise to stable oscillations.

Acknowledgment. This work has been supported by the EU Programme 'Improving the Human Research Potential and the Socio-Economic Knowledge Base' (Research Training Network Contract HPRN-CT-2000-00137).

References

[1] Andersson, N. (1998) A new class of unstable modes of rotating relativistic stars, *ApJ* **502** 708–713, gr-qc/9706075

[2] Arras, P., Flanagan, E. E., Morsink, S. M., Schenk, A. K., Teukolsky, S. A., Wasserman, I. (2002) Saturation of the R-mode Instability, *ApJ* Submitted, astro-ph/0202345

[3] Chandrasekhar, S. (1964) The dynamical instability of gaseous masses approaching the Schwarzschild limit in general relativity, *Phys. Rev. Lett.* **12** 114–116

[4] Font, J., Goodale, T., Iyer, S., Miller, M., Rezzolla, L., Seidel E., Stergioulas, N., Suen, W., Tobias, M. (2002) Three-dimensional general relativistic hydrodynamics II: long-term dynamics of single relativistic stars, *Phys. Rev. D* **65** 084024

[5] Lindblom, L., Tohline, J. E., Vallisneri, M. (2002) Numerical evolutions of nonlinear r-modes in neutron stars, *Phys. Rev. D* **65** 084039

[6] Oppenheimer, J. R., Snyder, H. (1939) On Continued Gravitational Contraction, *Phys. Rev.* **56** 455-459

[7] Schinder, P. J., Bludman, S. A., Piran, T. (1988) General-relativistic implicit hydrodynamics in polar-sliced space-time, *Phys. Rev. D* **37** 2722-2731

[8] Sperhake, U. (2001) *Non-linear numerical schemes in General Relativity,* PhD Thesis, University of Southampton, UK, gr-qc/0201086

[9] Sperhake, U., Papadopoulos, P., Andersson, N. (2001) Non-linear radial oscillations of neutron stars: Mode-coupling results, *MNRAS* Submitted, gr-qc/0110487

[10] Stergioulas, N., Font, J. A., Kokkotas, K. (1999) *Non-linear evolution of Rotating Relativistic Stars,* Contribution to the 19th Texas Symposium, gr-qc/9904009

[11] Van Hoolst, T. (1996) Effects of nonlinearities on a single oscillation mode of a star, *A&A* **308** 66-76